Molecular Biology of the Cell
Vol. 19, 722–734, February 2008

Munc18-1 Is Critical for Plasma Membrane Localization of Syntaxin1 but Not of SNAP-25 in PC12 Cells

Lakshmanan Arunachalam,[*†] Liping Han,[*†] Nardos G. Tassew,[‡] Yu He,[†§] Li Wang,[*] Li Xie,[†§] Yoshihito Fujita,[*] Edwin Kwan,[†§] Bazbek Davletov,[‖] Philippe P. Monnier,[†‡] Herbert Y. Gaisano,[*†§] and Shuzo Sugita[*†]

[*]Division of Fundamental Neurobiology and [‡]Division of Genetics and Development, Toronto Western Research Institute, University Health Network, Toronto, Ontario, M5T 2S8, Canada; Departments of [†]Physiology and [§]Medicine, Faculty of Medicine, University of Toronto, Ontario, M5S 1A8, Canada; and [‖]Medical Research Council, Laboratory of Molecular Biology, Cambridge CB2 2QH, United Kingdom

Submitted July 13, 2007; Revised October 31, 2007; Accepted November 29, 2007
Monitoring Editor: Benjamin Glick

Although Munc18-1 was originally identified as a syntaxin1–interacting protein, the physiological significance of this interaction remains unclear. In fact, recent studies of Munc18-1 mutants have suggested that Munc18-1 plays a critical role for docking of secretory vesicles, independent of syntaxin1 regulation. Here we investigated the role of Munc18-1 in syntaxin1 localization by generating stable neuroendocrine cell lines in which Munc18-1 was strongly down-regulated. In these cells, the secretion capability, as well as the docking of dense-core vesicles, was significantly reduced. More importantly, not only was the expression level of syntaxin1 reduced, but the localization of syntaxin1 at the plasma membrane was also severely perturbed. The mislocalized syntaxin1 resided primarily in the perinuclear region of the cells, in which it was highly colocalized with Secretogranin II, a marker protein for dense-core vesicles. In contrast, the expression level and the plasma membrane localization of SNAP-25 were not affected. Furthermore, the syntaxin1 localization and the secretion capability were restored upon transfection-mediated reintroduction of Munc18-1. Our results indicate that endogenous Munc18-1 plays a critical role for the plasma membrane localization of syntaxin1 in neuroendocrine cells and therefore necessitates the interpretation of Munc18-1 mutant phenotypes to be in terms of mislocalized syntaxin1.

INTRODUCTION

The Sec1-Munc18 (SM) proteins are essential proteins that regulate soluble *N*-ethylmaleimide–sensitive factor attachment protein receptor (SNARE) machineries by interacting with specific syntaxins and modulating the formation of the SNARE complex. In mammals there are seven SM proteins, of which the Munc18 isoforms-1, -2, and -3 (also called Munc18a, b, and c) are involved in exocytosis at the plasma membrane. Munc18-1 is predominantly expressed in the neurons and neuroendocrine cells (Hata *et al.*, 1993; Pevsner *et al.*, 1994), whereas Munc18-2 and -3 are more ubiquitously expressed (Hata and Südhof, 1995; Katagiri *et al.*, 1995; Tellam *et al.*, 1995; Halachmi and Lev, 1996; Riento *et al.*, 1996). Munc18-1 and -2 share binding preferences for syntaxin isoforms 1-3, whereas only Munc18-3 binds with syntaxin4 with high affinity (Hata and Südhof, 1995; Tellam *et al.*, 1995, 1997; Halachmi and Lev, 1996; Riento *et al.*, 1998, 2000; Kauppi *et al.*, 2002; Latham *et al.*, 2006; Hu *et al.*, 2007). Knockout of Munc18-3 leads to embryonic lethality (Kanda *et al.*, 2005; Oh *et al.*, 2005), whereas heterozygotic Munc18-3 knockout mice have impaired insulin sensitivity in an insulin tolerance test as well as defects in skeletal muscle insulin-stimulated GLUT4 translocation. Glucose-stimulated insulin secretion from islets isolated from the heterozygotic mice was also significantly compromised indicating the critical role for Munc18-3 in GLUT4 translocation in skeletal muscles and insulin secretion from pancreatic beta cells (Oh *et al.*, 2005).

The function of neuronal Munc18-1 and its orthologues has also been successfully examined through the analysis of null mutants. In these mutants, the release of neurotransmitter was reduced by ~85% in *Caenorhabditis elegans* and *Drosophila* (Hosono *et al.*, 1992; Harrison *et al.*, 1994) or completely blocked in mice (Verhage *et al.*, 2000), indicating Munc18-1's critical role in neurotransmitter exocytosis. However, *how* Munc18-1 contributes to exocytosis is poorly understood. Although Munc18-1 was originally identified as a syntaxin1-binding protein (Hata *et al.*, 1993; Pevsner *et al.*, 1994), the functional significance of this interaction remains elusive. Several hypotheses have been proposed regarding the role(s) for Munc18-1, including 1) docking factor of vesicles *in*dependent of syntaxin1 regulation (Voets *et al.*, 2001), 2) molecular chaperone of syntaxin1 for appropriate localization of syntaxin1 (Rowe *et al.*, 1999, 2001), 3) negative regulator of neurotransmitter release (Schulze *et al.*, 1994; Wu *et al.*, 1998), 4) regulator of fusion pores (Fisher *et al.*, 2001), and 5) activator of membrane fusion through its direct interaction with the SNARE complex (Zilly *et al.*, 2006; Dulubova *et al.*, 2007; Shen *et al.*, 2007).

Neurons from Munc18-1 knockout mice go through severe neurodegeneration and their morphological analysis

This article was published online ahead of print in *MBC in Press* (http://www.molbiolcell.org/cgi/doi/10.1091/mbc.E07–07–0662) on December 12, 2007.

Address correspondence to: Shuzo Sugita (ssugita@uhnres.utoronto.ca).

has thus been difficult (Verhage *et al.*, 2000; Heeroma *et al.*, 2004). After examination of the synapse at E14, the authors found no significant changes in vesicle docking at the synapse (Verhage *et al.*, 2000). However, they found a reduction (by ~85% of control) in the docking of dense-core vesicles in adrenal chromaffin cells (Voets *et al.*, 2001) from the knockout mice, and secretion from these cells was similarly reduced. Therefore, it was suggested that Munc18-1 promotes docking of dense-core vesicles and that undocked vesicles is the reason underlying the reduction in secretion. Recent analysis of *unc-18* mutants in *C. elegans* showed the reduction also in docking of synaptic vesicles at the synapse (Weimer *et al.*, 2003). Taken together, Munc18-1/*unc-18* is critical for docking of dense-core vesicles and may also regulate the docking of synaptic vesicles.

Munc18-1 is a soluble protein, implying that it regulates docking of dense-core vesicles by binding to the membrane protein(s) on the vesicles and/or the plasma membrane. In fact, the expression level of syntaxin1, an intrinsic transmembrane protein with which Munc18-1 interacts with, was reduced by ~50% in Munc18-1–deficient neurons and chromaffin cells (Voets *et al.*, 2001). A natural hypothesis resulting from these findings is that synatxin1 or other isoforms of syntaxin would control the docking of dense-core vesicles. Recently, viral infection of chromaffin cells with botulinum neurotoxin C1, which cleaves syntaxin1A, 1B, 2, and 3, was shown to reduce docking of dense-core vesicles strongly. This suggests that the plasma membrane syntaxins are indeed critical for docking of dense-core vesicles (de Wit *et al.*, 2006).

The hypothesis that Munc18-1 plays a role for syntaxin1 trafficking originated from exogenous transfection experiments; when exogenous syntaxin1 was transfected into fibroblasts, it remained stuck in the Golgi and/or the endoplasmic reticulum (ER; Rowe *et al.*, 1999; 2001). When Munc18-1 was cotransfected, syntaxin1 was distributed to the plasma membrane, the appropriate compartment for syntaxin1, suggesting that Munc18-1 helps to localize syntaxin1. *Surprisingly, however, this hypothesis has never been supported by loss-of-function studies of endogenous Munc18-1.* Namely, mislocalized syntaxin1 was not observed in Munc18-1–deficient neurons (Toonen *et al.*, 2005). This might be due to a difficulty of high-resolution immunocytochemistry of syntaxin1 in severely degenerated neurons from the knockout mice. Alternatively, Munc18-1 is important for the localization of syntaxin1 specifically in cells other than neurons (i.e., neuroendocrine cells). In any case, it remains unclear whether endogenous Munc18-1 is critical for plasma membrane localization of syntaxin1. Here we analyze the role for Munc18-1 in syntaxin1 localization in neuroendocrine PC12 cells using RNA interference-mediated down-regulation of Munc18-1.

MATERIALS AND METHODS

General Materials

Parental pSuper plasmid for knockdown constructs (Brummelkamp *et al.*, 2002) was a kind gift from Dr. Reuven Agami (Center for Biomedical Genetics, Netherlands). Plasmid pVenus-N1-NPY (Nagai *et al.*, 2002) was a kind gift from Dr. Atsushi Miyawaki (RIKEN, Wako, Saitama, Japan). Plasmid pBluescript-IRES-EGFP was a kind gift from Dr. Rafael Fernández-Chacón (University of Seville, Spain). This plasmid was originally constructed by Dr. Dagmar Pommereit in the laboratories of Drs. Christian Rosenmund (Max Planck Institute for Biophysical Chemistry) and Nils Brose (Max Planck Institute for Experimental Medicine, Germany). Plasmid pCMV-Emerald GFP was a kind gift from Dr. Weiping Han in Dr. Thomas Südhof's laboratory (University of Texas Southwestern Medical Center, Dallas, TX). Plasmid pBabe-puro (Brummelkamp *et al.*, 2002) and the plasmid containing human placental alkaline phosphatase cDNA were from Drs. Rod Bremner and Philippe Monnier (University Health Network, Canada). We obtained monoclonal antibodies against syntaxin1 (clone HPC-1) from Sigma (Oakville, ON, Canada); Munc18-1 from BD Bioscience (Mississauga, ON, Canada); SNAP-25 (clone SMI 81) and c-Myc (clone 9E10) from Covance (Berkeley, CA); polyclonal antibodies against Secretogranin II from QED Bioscience (San Diego, CA); and Calnexin from Sigma. mAb against SNAP-25 (Cl71.1) was a kind gift from Dr. Reinhard Jahn (Max Planck Institute for Biophysical Chemistry, Germany). Rabbit anti-Munc18-2 antibody (Riento *et al.*, 1998) and anti-VCP/p97 antibody (Sugita and Südhof, 2000) were kind gifts from Dr. Vesa Olkkonen (National Public Health Institute, Helsinki, Finland) and Dr. Thomas Südhof (University of Texas Southwestern Medical Center at Dallas), respectively.

Construction of Munc18-1 Knockdown Plasmids

To knockdown the rat Munc18-1 gene, we targeted the 19-nucleotide sequence of GTCTGTCCACTCTCTCATC (residues 246-264) in rat Munc18-1. We used TCTCTTGAA as a linker sequence. Sixty-four–base pair oligos containing sense and antisense of the target sequences were annealed and subcloned into the BamHI-HindIII sites of pSuper, generating the Munc18-1 knockdown plasmid (pSuper-rMunc18-1-3). Inserted sequences were verified by sequencing.

Isolation of Stable Munc18-1 Knockdown PC12 Cells

Wild-type PC12 cells (which were kind gifts from Dr. Thomas Martin, University of Wisconsin and Dr. Erik Schweitzer, University of California at Los Angeles) were maintained in DMEM (Invitrogen, Carlsbad, CA) containing 5% calf serum, 5% horse serum (both from Hyclone, Logan, UT), and penicillin/streptomycin (Sigma, St. Louis, MO; Wang *et al.*, 2004, 2005; Li *et al.*, 2005; Fujita *et al.*, 2007). To establish the Munc18-1 knockdown clone cells, PC12 cells were cotransfected with pSuper-rMunc18-1-3 (10 μg) and pBabe-puro (1 μg). We conducted two independent transfections: One transfection was achieved by electroporation (Li *et al.*, 2005; Fujita *et al.*, 2007) using linearized plasmids (for pSuper-rMunc18-1-3, SacI digestion; for pBabe-puro, NotI digestion), and the other was mediated by lipofection using FuGene6 (Roche, Laval, QC, Canada) with nonlinearized plasmids. Transfected cells were maintained in growth medium containing 2.5 μg/ml puromycin for more than a month. The growing colonies were picked up with pieces of Whatman paper soaked with Hanks' buffer containing 1 mM EDTA. Isolated colonies were grown in the growth medium without puromycin in 24-well plates. When the cells became confluent, they were transferred into two wells of six-well plates that contained the growth medium with 2.5 μg/ml puromycin. The cells in one of the six-well plates were subjected to immunoblot analysis using an anti-Munc18-1 mAb. Once the down-regulation of Munc18-1 was confirmed, the cells in the replica wells were transferred into 10-cm dishes containing the growth medium with puromycin. These cells were grown, frozen, and kept in a liquid nitrogen tank until use.

Real-Time PCR Quantification

Total RNA was isolated from cells using RNeasy kit (Qiagen, Chatsworth, CA) and quantified at OD 260/280 by spectrophotometer. cDNA was synthesized from 1 μg of total RNA using 200 U SuperScript III reverse transcriptase (Invitrogen) with 1× buffer, 500 μM each dNTP, and 50 μM oligo$(dT)_{20}$ primer in a 20-μl reaction volume. RNA was denatured at 65°C for 5 min with oligo$(dT)_{20}$ primer and dNTP before other components added, and then the reaction was carried at 50°C for 60 min followed by enzyme inactivation at 70°C for 15 min. RNA complementary was removed by incubation at 37°C for 20 min with 2 U of *Escherichia coli* RNase H. Real-time PCR was carried in ABI 7900HT (Applied Biosystems, Foster City, CA), with samples holding at 50°C for 2 min, 95°C for 10 min, and 40 cycles at 95°C for 15 s and 60°C for 1 min. A dissociation curve analysis was added immediately after the real-time cycles to confirm the specificity of the reaction. In a 10-μl reaction volume, 5 μl SYBR Green 2× master mix (Applied Biosystems) was applied with the cDNA and optimized primer condition (150 nM). Results were obtained by initial analysis by SDS 2.0 software package (Applied Biosystems) and further process according to the arithmetic formula (Fold difference = $2^{-}\Delta\Delta C_T$, $\Delta\Delta C_T = \Delta C_T$ test sample $- \Delta C_T$ calibrator sample) of the comparative C_T method ($\Delta\Delta$ C_T Method). GAPDH was used as the endogenous control. mRNA level of gene of interest was presented as the fold difference between the Munc18-1 knockdown (KD43) cells and the control (C1) cells. Primers used were as follows: syntaxin 1A forward, ACATGCTGGAGAGTGGGAAT; syntaxin1A reverse, ACTGTGCCTGGTCTCGATCT; syntaxin1B forward, TGGACTCGCAGATGACAAAG; syntaxin1B reverse, CAAACATGTCGTGCAGCTCT; Munc18-2 forward, AGGCCAACATCAAAGACCTG; Munc18-2 reverse, ATGCAGTCATCTGCCAAGTG; Munc18-1 forward TACGACCTGCTGCCTATTGA; Munc18-1 reverse, AGGTCATCGTCCTCATCCAG; GAPDH forward, CCCCACACACATGCACTTACC; and GAPDH reverse, CCTACTCCCAGGGCTTTGATT.

^{3}H-Norepinephrine Release Assays from PC12 Cells

PC12 cells were plated in 24-well plates; 3–4 d after plating, the cells were labeled with 0.5 μCi ^{3}H-Norepinephrine (NE) in the presence of 0.5 mM of

ascorbic acid for 12–16 h. The labeled PC12 cells were incubated with the fresh complete DMEM for 1–5 h to remove unincorporated [^{3}H]NE. The cells were washed once with physiological saline solution (PSS) containing 145 mM NaCl, 5.6 mM KCl, 2.2 mM $CaCl_2$, 0.5 mM $MgCl_2$, 5.6 mM glucose, and 15 mM HEPES, pH 7.4, and NE secretion was stimulated with 200 μl of PSS, high K^+-PSS (containing 81 mM NaCl and 70 mM KCl) or PSS containing 3 nM of α-latrotoxin (α-LTx; Alomone Labs, Jerusalem, Israel). Secretion was terminated after a 15-min (high K^+) or 10-min (α-Ltx) incubation at 37°C by chilling to 0°C, and samples were centrifuged at 4°C for 3 min. Supernatants were removed, and the pellets were solubilized in 0.1% Triton X-100 for liquid scintillation counting.

Electron Microscopy and Analysis of Docking of Dense-Core Vesicles

The initial fixation was performed within the 10-cm dishes for 1 h using a 3.2% glutaraldehyde, and 2.5% paraformaldehyde fixative mixture in 0.1 M cacodylate buffer (pH adjusted to 7.6). Cells were then pelleted in microcentrifuge tubes and fixed overnight with new fixative. The following day, the pellets were fixed in 1 mg/ml osmium tetroxide for 2 h and uranyl acetate for 1 h in dark conditions. Washed pellets were incubated successively in increasing concentrations of ethanol for dehydration purposes and then infiltrated with EPONAraldite plastic resin. The capsules containing the pellets were incubated for 48 h at 60°C, and the plasticized pellets were then sliced to ultrathin 80-nm sections, which were then mounted on copper grids for subsequent staining and viewing.

Grids mounted with the ultrathin cell sections were first etched by exposing the grids to uranyl acetate for 15 min at room temperature. Grids were then washed and stained with lead citrate for 20 min. Grids were washed and dried once again before loading onto Hitachi H7000 transmission electron microscope for viewing. Electron micrographs were taken of individual cells within each type of control or Munc18-1 knockdown clone. These images were then used for analyzing the docking of dense-core vesicles in the control or the Munc18-1 knockdown PC12 cells. Dense-core vesicles were identified within the single-cell electron micrographs as dark spots of radius between 60 and 120 nm. The distance of each vesicle from the plasma membrane was then calculated for each individual cell. The data from multiple single cell images (n = 14–46) within each control or Munc18-1 knockdown subclone has been collated.

Cell Preparation for Confocal Immunofluorescence Microscopy

Sterilized circular glass coverslips (0.25-mm width, 1.8-cm diameter) were placed in 2.2-cm wells within 12-well cell culture plates. The coverslips were then coated for 1 h with poly-D-lysine (0.1 mg/ml, Sigma) at room temperature. Both Munc18-1 knockdown and control PC12 cells were split onto the coated glass coverslips within each well. Cells were allowed to adhere to the coverslips overnight. In some cases, the PC12 cells were differentiated on the coverslips for 3–4 d in DMEM that contained 100 ng/ml nerve growth factor (NGF; Sigma), 1% horse serum, 1% calf serum, and penicillin/streptomycin. The cells were washed with phosphate-buffered saline (PBS), fixed for 15 min with PBS containing 4% paraformaldehyde, and permeabilized with PBS containing 0.2% Triton X-100 and 0.3% bovine serum albumin (BSA) for 5 min or PBS containing 0.05% Triton X-100 and 3% goat serum for 1 h. Nonspecific sites were blocked for 1 h at room temperature in PBS containing 0.3% BSA or PBS containing 0.05% Triton X-100 and 3% goat serum. Primary antibodies against syntaxin1 (HPC-1 diluted 1:500), SNAP-25 (Cl71.1 diluted 1:500), Secretogranin II (rabbit polyclonal antiserum diluted 1:1000), or Calnexin (rabbit polyclonal antiserum diluted 1:1000) were diluted in blocking buffer and applied to the permeabilized cells for 1 h at room temperature or overnight at 4°C. After three washes in blocking buffer, Alexa 488–conjugated goat anti-mouse antibodies (diluted 1:1000), Alexa 568–conjugated goat anti-rabbit antibodies (diluted 1:1000; both from Invitrogen) or red-x–conjugated anti-mouse antibodies (diluted 1:1000; Jackson ImmunoResearch, West Grove, PA) were diluted in blocking buffer and applied for 1 h at room temperature. Samples were washed again three times in blocking buffer and mounted in Fluoromount-G reagent (Southern Biotechnology Associates, Birmingham, AL). Immunofluorescence staining was recorded with a Zeiss laser confocal scanning microscope (LSM 510; Thornwood, NY) with an oil immersion objective lens (63×).

Confocal Microscope Image Acquisition and Data Analysis

Images were taken from undifferentiated single cells at an appropriate scale to allow the subsequent numerical analysis. The images of single cells were split into two regions during the analysis representing the plasma membrane and intracellular compartments of the cell. The regional split was attained through tracing the outlines of the plasma membrane on either side of the cell. Such tracings were possible as both syntaxin1 and SNAP-25 have plasma membrane localization within the cells. The intensity of all pixels within each region was summed to obtain a net intensity for each region. To accommodate differences in cell sizes within the samples, the net intensity of both regions were divided by the area of the respective regions. The area of a region was estimated by calculating the net number of pixels within that region. This area-normalized intensity then allowed an analysis of the localization of the different proteins studied. In representing localization the following localization ratio was calculated as follows: Area − Normalized Intensity of Plasma Membrane Compartment/Area − Normalized Intensity of Intracellular Compartment. The magnitude of the localization ratio represents the strength of the plasma membrane localization relative to intracellular regions for specific proteins analyzed.

Equilibrium Sucrose Density Gradient

Two dishes each of control (C1) and Munc18-1 knockdown (KD43) cells were detached from the dishes by a 3-min incubation with 1 ml Hanks' buffer containing 1 mM EDTA at 37°C. Seven milliliters of complete growth medium was added, and the cells were harvested in a 15-ml tube. The harvested cells were pelleted by centrifugation, resuspended in 1 ml of homogenization buffer (250 mM sucrose, 1 mM $MgCl_2$, 0.005% DNAse, 4 mM HEPES-NaOH, pH 7.4, and the following protease inhibitors: 0.4 mM PMSF, 10 mM benzamidine, 4 μg/ml each of pepstatin A, leupeptin, antipain, and aprotinin; Reetz *et al.*, 1991). The resuspended cells were passed 10 times through a ball homogenizer (clearance: 0.0004 inches = ~10 μm). The homogenized cells were centrifuged by 5000 × *g* for 10 min, and the supernatant (PNS, post nuclear supernatant) was recovered. EDTA was added to PNS to a final concentration of 1.5 mM. The PNS was loaded onto the top of a 3.2 ml of continuous sucrose gradient (0.60–2 M sucrose) in a SW60Ti rotor and centrifuged at 32,900 rpm for 18 h at 4°C. Fractions (257 μl each) were collected from the top of the gradient and mixed with one-fifth volume of 6× Laemmli sample buffer. Fractions (20 μl) were then analyzed by SDS-PAGE and immunoblotting.

Munc18-1 Expression Constructs

To protect the mRNA transcripts transcribed from the Munc18-1 expression plasmid from being degraded by the anti-Munc18-1 RNA interference machineries already induced within the Munc18-1 knockdown cells, we introduced six silent nucleotide mutations (SNMs; GTCCGTGCACAGCCTGATC; underlines indicate SNM) within the target sequence in the Munc18-1 gene. The resulting Munc18-1 gene was subcloned within pCMV5 plasmid (Sugita *et al.*, 1999). The Munc18-1 gene was also attached to the sequence of IRES (internal ribosome entry site) enhanced green fluorescent protein (EGFP). The IRES allows EGFP to be produced from the same mRNA transcript as Munc18-1, therefore serving as a reporter to indicate transfected cells that could then be imaged. This construct, named pCMV-Munc18-1(SNM)-IRES-EGFP, was made by subcloning the SalI-XbaI fragment from pBluescript-IRES-EGFP into the same site in pCMV-Munc18-1(SNM). We also generated the construct that expresses Munc18-1(SNM) as an Emerald GFP fusion protein. This construct, pCMV-Munc18-1(SNM)-Emerald GFP, was made as follows: 0.7-kb BglII/BamHI fragment of pCMV-Emerald GFP was subcloned into BamHI site of pCMV5 generating pCMV-Emerald GFP-2. A 1.8-kb PCR product containing full-length Munc18-1(SNM) without a stop codon was digested with EcoRI/HindIII and subcloned into the same site of pCMV-Emerald GFP-2.

Munc18-1 Transfection to Rescue Syntaxin1 Mislocalization

The Munc18-1 knockdown cells were transfected with pCMV-Munc18-1(SNM)-IRES-EGFP by electroporation and stained with anti-syntaxin1 antibody, followed by red-x–conjugated goat anti-mouse antibodies. The syntaxin1 localization analysis protocol was then applied to these single cell images, and the localization ratios obtained for the cells expressing EGFP were compared with that of cells not expressing EGFP. We also differentiated Munc18-1 knockdown cells transfected with pCMV-Munc18-1(SNM)-IRES-EGFP or pCMV-Munc18-1(SNM)-Emerald GFP by NGF. These cells were stained with anti-syntaxin1 or SNAP-25 antibody followed by red-x–conjugated goat anti-mouse antibodies. Images that contain both transfected and untransfected cells were acquired to allow the direct comparison of sytaxin1 or SNAP-25 staining between the transfected and untransfected cells.

hPLAP Secretion Assay from PC12 Cells

We constructed a reporter plasmid (pCMV-NPY-hLAP) that enables the expression of neuropeptide-Y fused with a soluble domain of human placental alkaline phosphatase (residues 18–506). This plasmid was generated by replacing the Venus sequence of pVenus-N1-NPY (Nagai *et al.*, 2002) with cDNA, which encodes the soluble domain of hPLAP that was amplified by PCR. PC12 cells at 70–80% confluency in 10-cm dishes were cotransfected with 3 μg of pCMV-hPLAP and 10 μg of empty pCMV5 (for control) or pCMV-Munc18-1(SNM; for rescue) using electroporation. After 48 h, the cells were harvested and replated in 24-well plates. Six or 7 d after electroporation, the plated cells were washed once with PSS, and NPY-hPLAP secretion was stimulated with 200 μl of PSS or high K^+-PSS. Secretion was terminated after a 20-min incubation at 37°C by chilling to 0°C, and samples were centrifuged at 4°C for 3 min. Supernatants were removed, and the pellets were solubilized in 200 μl PSS containing 0.1% Triton X-100. The amounts of NPY-hPLAP secreted into the medium and retained in the cells were measured by the

Phospha-Light Reporter Gene Assay System (Applied Biosystems). We treated the samples at 65°C for 30 min to inactivate nonplacental alkaline phosphatases and assayed an aliquot (10 μl) for placental alkaline phosphatase activity with the kit. The total volume of the assay was 120 μl. After 5–10 min, chemiluminescence was quantified by FB12 luminometer (Berthold Detection Systems, Zylux Corporation, Oak Ridge, TN).

RESULTS

Generation of Stable Munc18-1 Knockdown Cells

To examine the function of Munc18-1, including its role in syntaxin1 trafficking, we generated stable PC12 cell lines in which the expression of Munc18-1 was strongly down-regulated by RNA interference. Highly significant reductions in Munc18-1 levels within knockdown cells were crucial toward the establishment of such knockdown cells as possible replacements to the knockout cell models. We cotransfected PC12 cells with the plasmid that expresses a short-hairpin RNA against rat Munc18-1 mRNA (pSuper-rMunc18-1-3) and a plasmid that confers puromycin resistance (pBabe-puro). Independent colonies of stable transfectants of PC12 cells were isolated after incubation with puromycin for over a month. Clones isolated from selection plates were subsequently analyzed for their effectiveness in knocking down Munc18-1. Western blots revealed a variation in the Munc18-1 levels among different knockdown clones. Control clones were similarly isolated by using an empty pSuper plasmid (instead of pSuper-rMunc18-1-3) that was cotransfected with pBabe-puro. At no time did we observe a reduction of Munc18-1 expression in the control clones. Eight of the Munc18-1 knockdown clones with the lowest levels of Munc18-1 expression paired with control clones are shown in the immunoblot in Figure 1A. The levels of Munc18-1 expression within the knockdown clones were decreased by approximately more than 90% when compared with Munc18-1 levels within control cells.

We also examined the expression level of isoforms of Munc18-1, namely Munc18-2 and -3 (Hata and Südhof, 1995; Katagiri *et al.,* 1995; Tellam *et al.,* 1995; Halachmi and Lev, 1996; Riento *et al.,* 1996; Figure 1A). Interestingly, we not only detected the expression of Munc18-2 in the control and knockdown PC12 clones but also the apparent up-regulation of Munc18-2 in the knockdown clones for six of the eight pairs (Figure 1A). We quantified the difference in Munc18-2 protein expression for each pair using VCP/p97, a ubiquitous membrane-trafficking protein (Peters *et al.,* 1990) as a loading control. We found an increase of 27.2 ± 12.5% (mean ± SEM, n = 8) in Munc18-2 protein expression for Munc18-1 knockdown cells, but this up-regulation was not statistically significant due to some variability between cell lines (paired Student's *t* test, $t_7 = 2.19$, $p = 0.065$; Figure 1B). This potential up-regulation of Munc18-2 may be a compensatory response to the knockdown of Munc18-1. A similar compensatory increase was previously observed in the expression of cellubrevin, a close isoform of synaptobrevin 2, in the synaptobrevin 2 knockout chromaffin cells (Borisovska *et al.,* 2005). The expression of Munc18-3 was so low that we could not clearly detect its presence by the antibody used, but the expression level appeared to be unaffected by Munc18-1 knockdown (data not shown).

We then examined the expression of syntaxin1, a SNARE protein that interacts with Munc18-1 (Hata *et al.,* 1993; Garcia *et al.,* 1994; Pevsner *et al.,* 1994), along with SNAP-25, another t-SNARE protein (Sollner *et al.,* 1993). As was the case in the neurons and chromaffin cells from Munc18-1 knockout mice (Verhage *et al.,* 2000; Voets *et al.,* 2001; Toonen *et al.,* 2005), a decrease in syntaxin1 levels was consistently observed within our Munc18-1 knockdown PC12 cells albeit to a much lesser extent (14.0 ± 3.7% decrease, n = 8; Figure 1, A and B). This decrease was statistically significant when quantified using VCP/p97 as a loading control ($t_7 = 3.89$, $p < 0.01$; Figure 1B). The more modest reduction of syntaxin1 in the knockdown cells is presumably because the residual expression of Munc18-1 is sufficient to support better expression of syntaxin1 than in the knockout cells. Significant expression and compensatory up-regulation of Munc18-2 in the knockdown cells may also support the better expression of syntaxin1. The plasticity in syntaxin1 expression is an indication of the strong physiological significance of the functional interaction between Munc18-1 and syntaxin1. This establishes the functional comparability between our Munc18-1 knockdown PC12 model and the secretory cells from Munc18-1 knockout mice. No decrease in SNAP-25 expression was detected for Munc18-1 knockdown cells (Figure 1, A and B), thereby warranting the specificity in the reduction of syntaxin1.

Significant decreases in syntaxin1 expression and potential increases in Munc18-2 expression in the Munc18-1 knockdown cells could be mediated at the transcription level or at the posttranslational level. To detect any regulation of protein expression at the transcriptional level, we quantified mRNA of syntaxin1A, syntaxin1B, and Munc18-2, as well as Munc18-1 in Munc18-1 knockdown (KD43) and control (C1) cells using quantitative real-time RT-PCR. We originally thought that down-regulation of syntaxin1 is mediated at the posttranscriptional level. That is, syntaxin1 would be generated normally but be degraded more rapidly in the absence of Munc18-1. Unexpectedly, however, we found decreases in mRNA of syntaxin1A and 1B in the knockdown cells. On the other hand, there was an increase in mRNA of Munc18-2 in these cells (Table 1). These results suggest that changes in expression level of these proteins are regulated at least in part at the transcription level. mRNA of Munc18-1 is down-regulated by >95% in the knockdown cells confirming our efficient knockdown of Munc18-1 (Table 1).

Secretion Defects and Reduction in Docking of Dense-Core Vesicles in the Munc18-1 Knockdown Cells

As was the case in the chromaffin cells from Munc18-1 knockout mice, we found that the secretory ability of the Munc18-1 knockdown cells was significantly diminished in comparison to control cells. Secretion analyses were performed on the eight Munc18-1 knockdown clones and their paired controls shown in Figure 1A. Figure 1B shows the average of multiple (n = 9) secretion assays for each pairs of the clones stimulated by 70 mM KCl. Figure 1C shows the average of multiple (n = 9) secretion assays for the same clones; however, in this case the cells were stimulated using 3 nM α-LTx. All secretion percent values shown were normalized to that of the average secretion of the paired control cells under high K^+ (Figure 1C) or α-LTx (Figure 1D). Secretion was consistently decreased in knockdown clones by 40–70% in both the high K^+ and α-LTx induction experiments when compared with control clones. The results clearly indicate that the defects in high K^+-induced secretion are not the result of defects upstream of Ca^{2+}-influx after high K^+-induced depolarization but rather are due to defects in the secretion machineries themselves.

We also examined the docking of dense-core vesicles through electron microscopy. Here we use the term "docking" as the anatomical definition to refer to the phenomenon of secretory vesicles in close apposition (within 50 nm) to the plasma membrane. We found a significant decrease in the proportion of docked dense-core vesicles within the Munc18-1 knockdown PC12 cells. Such vesicle docking defects have in

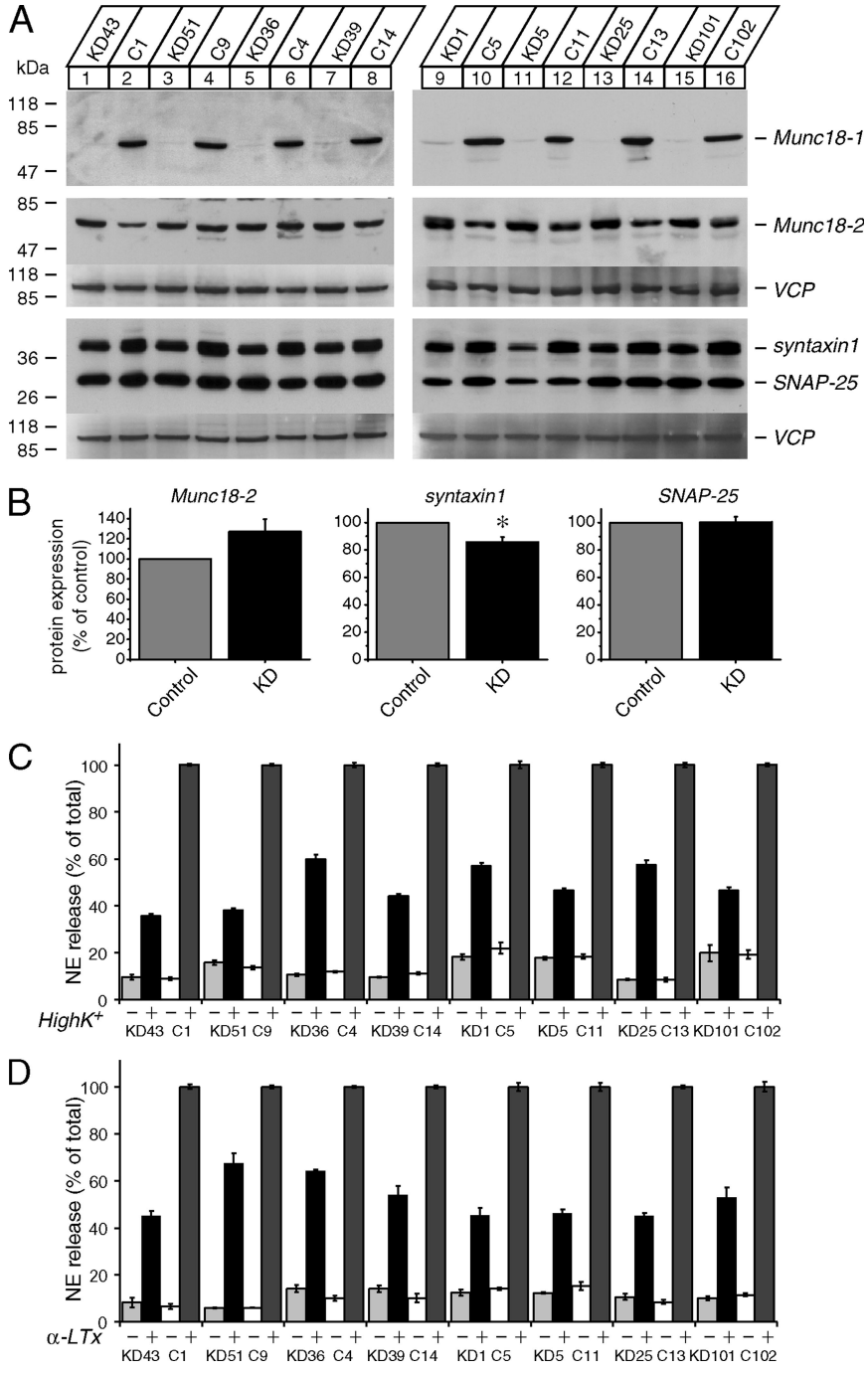

Figure 1. Down-regulation of Munc18-1 results in secretion defects. (A) Immunoblot analysis of multiple Munc18-1 knockdown cells. Thirty micrograms of total homogenates from the Munc18-1 knockdown (KD) and control (C) cells were analyzed by SDS-PAGE and immunoblotting using anti-Munc18-1, -2, syntaxin1, SNAP-25, and antibodies. The signal was detected with enhanced chemiluminescence detection system. The membranes used for the analysis of Munc18-2, syntaxin1, and SNAP-25 were reprobed with polyclonal antibody against VCP/p97 (used as a loading control). Numbers on the left indicate positions of molecular-weight markers. (B) Quantification of changes in protein expression of Munc18-2, syntaxin1, and SNAP-25 between control and Munc18-1 knockdown cells. Images of these proteins on the film were quantified with Luminescent Image Analyzer (Fuji Film, Tokyo, Japan; LAS-3000) and normalized with the signals of VCP. The protein expression in the knockdown cells was further normalized with that in paired control cells ($n = 8$). *$p < 0.01$; a statistically significant difference. (C) NE release was stimulated by 70 mM KCl for 15 min. Eight pairs of knockdown and control clones were examined. Error bars, SEM ($n = 9$). (D) NE release was stimulated by 3 nM α-latrotoxin for 10 min. Eight pairs of knockdown and control clones were examined. Error bars, SEM ($n = 9$).

fact been already observed in both Munc18-1 knockout mice chromaffin cells (Voets *et al.*, 2001) and *unc-18* null-mutant *C. elegans* (Weimer *et al.*, 2003). Representative electron micrograph for a Munc18-1 knockdown (KD43) cell is shown in Figure 2A along with that of a control (C9) PC12 cell (Figure 2B). Docked dense-core vesicles are indicated by open arrowheads and undocked dense-core vesicles are indicated by closed arrows. A summary of the dense-core vesicle docking analysis is represented in Figure 2C. In both knockdown clones there is ~50% decrease in the proportion of docked vesicles (found within 50 nm of the plasma membrane) when compared with control clones. This difference was statistically significant based on one-way ANOVA ($F = 17.7$, $p < 0.01$) followed by post hoc test. This lack of proximity between the dense-core vesicles and the plasma membrane suggests deficiencies in vesicle docking among the Munc18-1 knockdown clones. Although we found considerable variation in the total number of dense-core vesicles per cell among clones, no consistent differences were noted between the knockdown and control populations (Figure 2D).

Syntaxin1, But Not SNAP-25, Is Mislocalized in the Munc18-1 Knockdown Cells

To elucidate the role for Munc18-1 in syntaxin1 localization, we examined syntaxin1 immunostaining using monoclonal anti-syntaxin1 antibody (HPC-1; Barnstable *et al.*, 1985) in

Table 1. Analysis of fold change expression of mRNA by real-time quantitative RT-PCR, calculated by the $\Delta\Delta C_T$ method

Sample	Gene name	Protein average C_T	GAPDH average C_T	ΔC_T Protein − GAPDH	$\Delta\Delta C_T$ ΔC_T protein − ΔC_T control	Fold difference in Protein relative to control
Control 1	Syntaxin1A	29.91 ± 0.01	18.73 ± 0.02	11.32 ± 0.00	0.00 ± 0.00	1 (1–1)
KD43	Syntaxin1A	29.45 ± 0.06	18.13 ± 0.07	11.18 ± 0.00	0.14 ± 0.00	0.9 (0.9–0.9)
Control 1	Syntaxin1B	30.90 ± 0.11	18.73 ± 0.02	12.17 ± 0.07	0.00 ± 0.07	1 (1–1)
KD43	Syntaxin1B	30.89 ± 0.17	18.13 ± 0.07	12.77 ± 0.07	0.60 ± 0.07	0.6 (0.6–0.6)
Control 1	Munc18-2	30.08 ± 0.03	18.73 ± 0.02	11.35 ± 0.00	0.00 ± 0.00	1 (1–1)
KD43	Munc18-2	29.17 ± 0.05	18.13 ± 0.07	11.04 ± 0.01	−0.31 ± 0.01	1.2 (1.2–1.2)
Control 1	Munc18-1	24.31 ± 0.02	18.73 ± 0.02	5.58 ± 0.00	0.00 ± 0.00	1 (1–1)
KD43	Munc18-1	28.53 ± 0.14	18.13 ± 0.07	10.40 ± 0.06	4.82 ± 0.06	0.03 (0.03–0.03)

the knockdown and control cells. A representative image of syntaxin1 staining from four pairs of knockdown and control clones is presented in Figure 3, A and B. In control cells, strong syntaxin1 staining at the plasma membrane was detected (Figure 3B). A more significant staining of intracellular organelles and the concomitant reduction in plasma membrane staining was observed in all the Munc18-1 knockdown PC12 cells (Figure 3A). We then quantified the syntaxin1 mislocalization through pixel intensity localization analysis (see *Materials and Methods*). A summary of the syntaxin1 localization analysis for four different pairs of knockdown and control clones are shown in Figure 3C. We noted a significant decrease (by ~30–50% compared with control) in the localization ratio of plasma membrane syntaxin1 versus syntaxin1 in the cytoplasm of the cells among the Munc18-1 knockdown clones in comparison to control clones (Student's *t* test, $t_6 = 7.78$, $p < 0.01$). This would indicate that Munc18-1 knockdown caused significant mislocalization of syntaxin1 in intracellular compartments away from the plasma membrane.

The localization of SNAP-25 was also analyzed similarly and was found to be no different in Munc18-1 knockdown cells compared with controls. Examples of individual confocal images of the knockdown and control clones are shown in Figure 4, A and B. A summary of SNAP-25 localization analysis for the same four Munc18-1 knockdown clones and control clones are shown in Figure 4C. The lack of SNAP-25 mislocalization within Munc18-1 knockdown clones (Student's *t* test, $t_6 = 0.34$) confirms the specific mislocalization of syntaxin1 alone rather than a general mislocalization of plasma membrane proteins. The specific syntaxin1 mislocalization upon Munc18-1 knockdown suggests a role for Munc18-1 in the proper localization of syntaxin1.

Syntaxin1 Resides in the Perinuclear Region in Undifferentiated and NGF-differentiated Knockdown Cells

We attempted to identify the precise localization of misplaced syntaxin1 in Munc18-1 knockdown PC12 cells. For this purpose, we first conducted three-dimensional analyses of syntaxin1 staining in the Munc18-1 knockdown (KD43) and control (C1) cells. Multiple confocal images along Z-axis were captured and stacked together to reconstitute three-dimensional images of syntaxin1 staining. Such an example

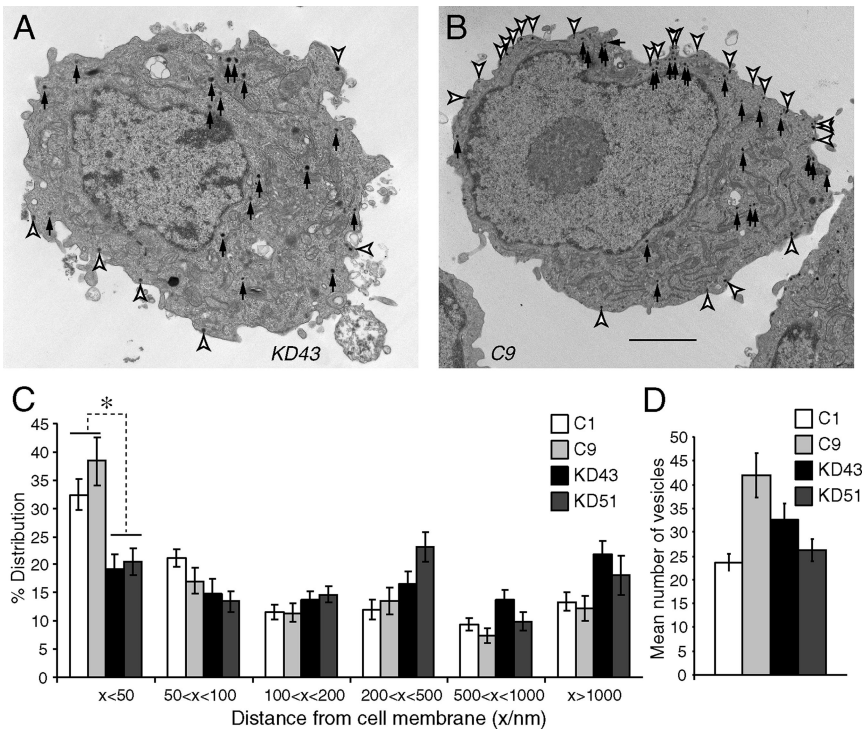

Figure 2. Electron microscopy of the Munc18-1 knockdown cells reveals abnormalities in the docking of dense-core vesicles. (A and B) Electron micrograph of single cell from Munc18-1 knockdown (KD43) clone (A) and control (C9) clone (B). Docked dense-core vesicles are indicated by open arrowheads and undocked dense-core vesicles are indicated by closed arrows. Scale bar, 1 μm. (C) The graph shows the mean percentage distribution of dense-core vesicles within individual PC12 cells, calculated from multiple single-cell electron micrographs from four different clones. Dense-core vesicles were classed as being located within 50, 50–100, 100–200, 200–500, and 500–1000 nm, as well as farther than 1000 nm from the plasma membrane. *$p < 0.01$; a statistically significant difference. Error bar, SEM (n = 14–26). (D) The graph shows mean number of vesicles present in each single-cell electron micrograph from the four different clones (two Munc18-1 knockdown clones and two control clones). Error bar, SEM (n = 14–26).

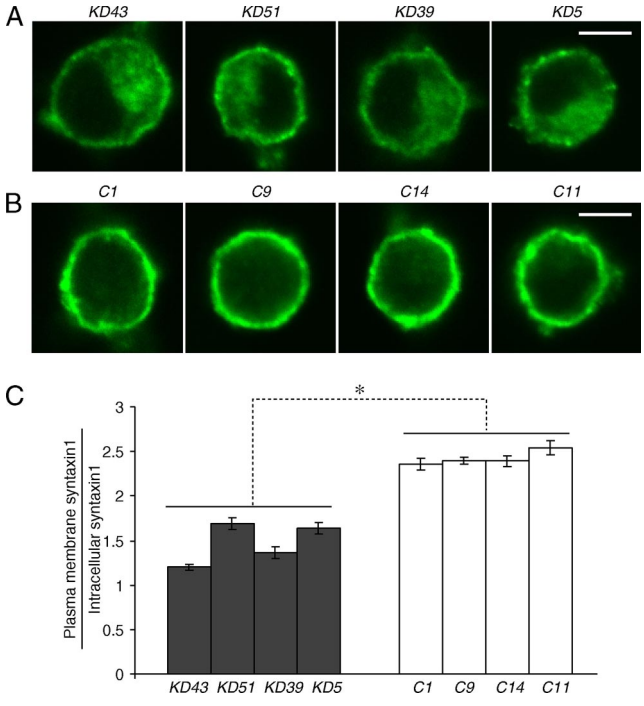

Figure 3. Confocal immunofluorescence microscopy reveals syntaxin mislocalization in Munc18-1 knockdown cells. (A and B) Representative single-cell confocal images of cells from four pairs of knockdown (A) and control (B) that were stained by anti-syntaxin1 antibodies (HPC-1) followed by Alexa 488–conjugated anti-mouse antibodies. Scale bar, 5 μm. (C) The graph shows the proportion of syntaxin1 found in the plasma membrane to that found inside the cell for four pairs of knockdown clones and their paired controls. Error bar, SEM (n = 14–26). *p $<$ 0.01; a statistically significant difference.

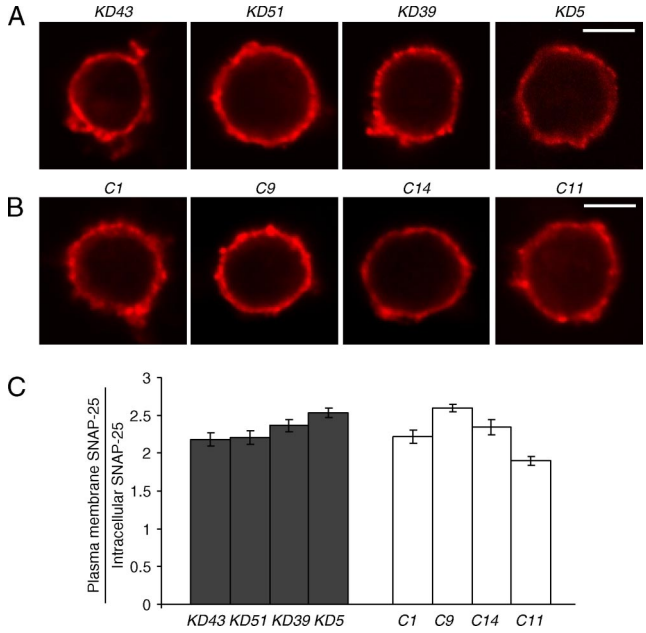

Figure 4. Unchanged SNAP-25 localization in Munc18-1 knockdown cells. (A and B) Representative single-cell confocal images of cells from four pairs of knockdown (A) and control (B) cells that were stained with anti-SNAP-25 monoclonal antibodies (Cl71.1), followed by red-x–conjugated goat anti-mouse antibodies. Scale bar, 5 μm. (C) The figure shows the proportion of SNAP-25 found in the plasma membrane to that found inside the cell for two different knockdown clones and their paired controls. Error bar, SEM (n = 12–19).

for KD43 and C1 cells are presented as Supplementary Materials (Supplementary Movies 1 and 2). As shown in these images, syntaxin1 staining was accumulated near the perinuclear region in the knockdown cell. In contrast, anti-syntaxin antibody stained the surface of the control cells.

The size of undifferentiated PC12 cells is relatively small ($<$10 μm in diameter) and this makes it difficult to identify the exact localization of each organelle. To better localize each organelle, we differentiated PC12 cells using NGF. The cell bodies of differentiated PC12 cells enlarge and become flatter, which allows us to better examine colocalization of misplaced syntaxin1 with organelle marker proteins. After a 4-d treatment with NGF (100 ng/ml), both the knockdown and control cells exhibited normal neurite outgrowth. In the differentiated Munc18-1 knockdown (KD43) cells, staining with syntaxin1 antibody showed marked perinuclear staining (Figure 5A), whereas in control (C1) cells, it showed clear plasma membrane staining (Figure 5B). Because differentiated cells become flatter, the optical sectioning by confocal microscopy is more consistent among many cells, and we could observe very consistent phenotypic differences between knockdown and control cells under NGF-differentiated conditions.

We then analyzed the localization of misplaced syntaxin1 in the somata with higher magnifications and examined its colocalization with the three marker proteins: GM130 (a marker protein for the *cis*-Golgi), Calnexin (a marker protein for the ER), and Secretogranin II (a marker protein for dense-core vesicles; Figure 6). Calnexin staining was reduced at the pe-

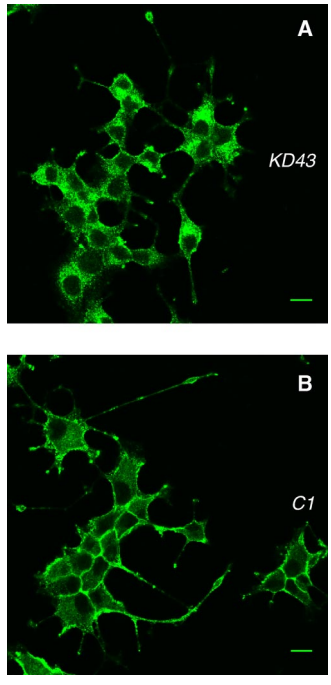

Figure 5. Mislocalized syntaxin1 accumulates in the perinuclear region of the cells in NGF-differentiated Munc18-1 knockdown cells. NGF-differentiated Munc18-1 knockdown (KD43; A) cells and control (C1; B) were stained with anti-syntaxin1 monoclonal antibodies followed by Alexa 488–conjugated goat anti-mouse antibodies. Scale bar, 10 μm.

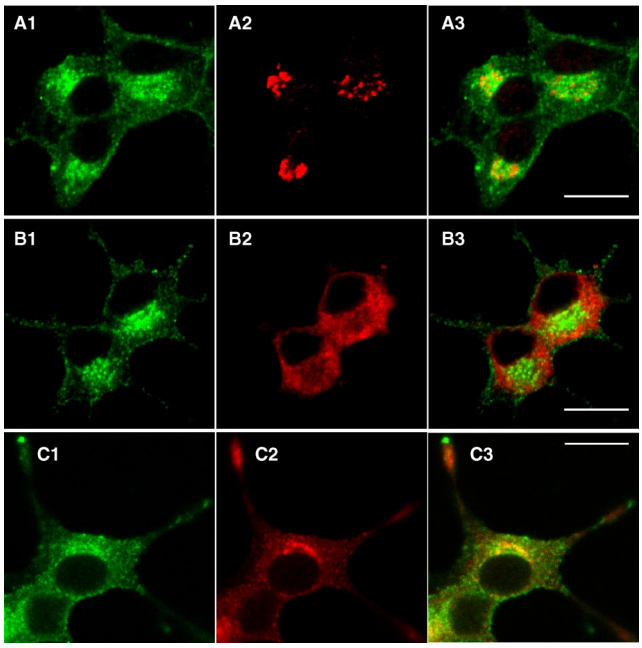

Figure 6. Misplaced syntaxin1 is enriched on the dense-core vesicles in the perinuclear region of the cells in the somata of NGF-differentiated Munc18-1 knockdown cells. NGF-differentiated Munc18-1 knockdown (KD43) cells were costained with anti-syntaxin1 monoclonal antibodies (A1–C1) followed by Alexa 488–conjugated goat anti-mouse antibodies, and anti-GM-130 rabbit polyclonal antibody (A2), anti-calnexin rabbit polyclonal antibody (B2), or anti-Secretogranin II rabbit polyclonal antibodies (C2) followed by Alexa 568–conjugated goat anti-rabbit antibodies. Light panels (A3–C3) are merged pictures. Note the highest colocalization was observed between sytaxin1 and Secretogranin II (C3). Scale bar, 10 μm.

rinuclear region (Figure 6B2) and showed a marked contrast to the syntaxin1 staining (Figure 6B1), indicating that syntaxin1 is not on the ER. In contrast, the perinuclear enrichment was observed in the staining with anti-GM130 (Figure 6A2) and anti-Secretogranin II (Figure 6C2) antibodies. Different from GM-130 staining, which exhibited Golgi-ribbon patterns, the syntaxin1 staining showed punctuate patterns, which was more similar to Secretogranin II staining (Figure 6C). Thus, at least a portion of the misplaced syntaxin1 appeared to be localized on dense-core vesicles in the perinuclear region. Considering the fact that the biogenesis of dense-core vesicles is initiated in the *trans*-Golgi network (Tooze, 1998), our results suggest that misplaced syntaxin1 is stuck on the membrane structures between the Golgi and the plasma membrane, which include dense-core vesicles. Thus, without Munc18-1, the trafficking of syntaxin1 from the *trans*-Golgi to the plasma membrane is severely perturbed.

We also examined the localization of SNAP-25 in the NGF-differentiated PC12 cells. Plasma membrane staining is similarly prominent both in the knockdown and control cells (Figure 7), confirming that down-regulation of Munc18-1 did not affect SNAP-25 localization in the differentiated PC12 cells. We suggest that without Munc18-1, syntaxin1 trafficking from the ER to the plasma membrane is rendered inefficient, whereas the trafficking of SNAP25 remains unaffected.

Subcellular Fractionation Reveals Changes in Distribution of Syntaxin1 in Munc18-1 Cells

Although we found very consistent mislocalization of syntaxin1 in Munc18-1 knockdown cells by immunofluorescence confocal microscopy, we wanted to confirm the above using an independent approach. Toward this end, we performed subcellular fractionation using equilibrium sucrose gradients. Postnuclear supernatants from control (C1) and knockdown (KD43) cells were loaded onto the top of a continuous sucrose density gradient and centrifuged. In Western blotting analyses, we found that in control cells,

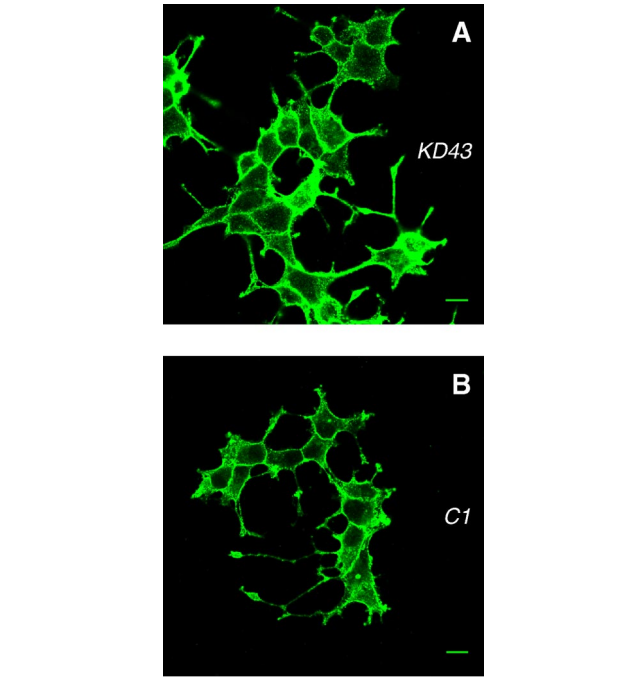

Figure 7. Unchanged plasma membrane localization of SNAP-25 in NGF-differentiated Munc18-1 knockdown cells. Munc18-1 knockdown (KD43; A) and control (C1; B) cells were stained with monoclonal anti-SNAP-25 antibody followed by Alexa 488–conjugated goat anti-mouse antibody. Scale bar, 10 μm.

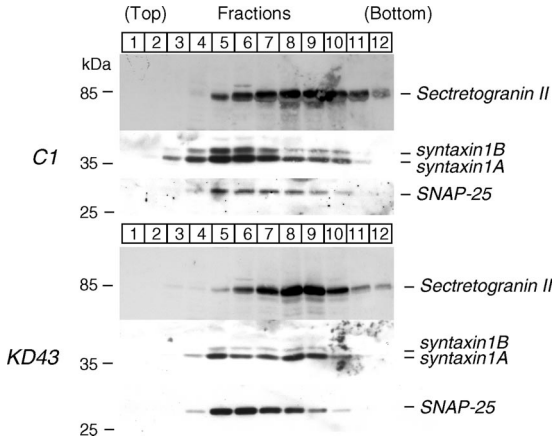

Figure 8. Fractionation of control (C1) cells and Munc18-1 knockdown (KD43) cells reveals changes in distribution of syntaxin1. Postnuclear supernatants of total homogenates of C1 and KD43 cells were loaded onto a continuous 0.60–2 M sucrose gradient. Fractions were collected from the top and equal volumes of such fractions were analyzed by SDS-PAGE and immunoblotting with anti-Secretogranin II, syntaxin1, and SNAP-25 antibodies. The number on the blots indicates the position of fractions. Molecular weights in kDa are indicated in the left.

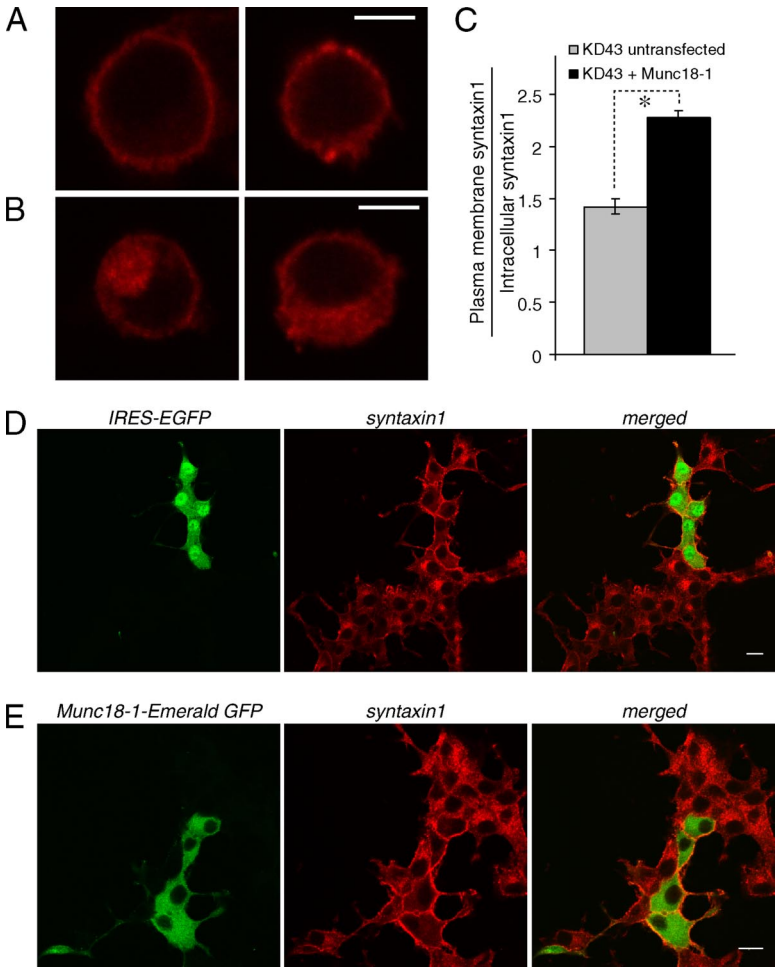

Figure 9. Rescue of Syntaxin1 localization upon reintroduction of Munc18-1 into KD43 cells. (A and B) Representative single-cell confocal images of KD43 cells that were transfected with pCMV-Munc18-1(SNM)-IRES-EGFP (A) as well as untransfected KD43 cells (B), both stained for anti-syntaxin1 antibodies followed by red-x–conjugated anti-mouse antibodies. Transfected cells were identified through the expression of IRES-EGFP. Scale bar, 5 μm. (C) Summarized figure shows the proportion of syntaxin1 found in the plasma membrane to that found inside the cell for KD43 cells transfected with pCMV-Munc18-1(SNM)-IRES-EGFP as well as untransfected KD43 cells. Error bar, SEM (n = 16). *$p < 0.01$; a statistically significant difference. (D) Confocal images of NGF-differentiated multiple KD43 cells transfected with pCMV-Munc18-1(SNM)-IRES-EGFP that were stained with anti-syntaxin1 monoclonal antibodies followed by red-x–conjugated goat anti-mouse antibodies. (E) Confocal images of NGF-differentiated KD43 cells transfected with pCMV-Munc18-1(SNM)-Emerald GFP that were stained with anti-syntaxin1 monoclonal antibodies followed by red-x–conjugated goat anti-mouse antibodies. Scale bar, 10 μm.

dense-core vesicle marker Secretogranin II shows highest level of presence in fractions 8 and 9, whereas syntaxin1 and SNAP25 are in fractions 5 and 6 (Figure 8). These results suggest that syntaxin1 and Secretogranin II fractions can be largely separable using this technique. Furthermore, the cofractionation of syntaxin1 and SNAP-25 in control cells confirms the data that show their colocalization in the plasma membrane. In Munc18-1 knockdown cells, fraction patterns were the same as in control cells for Secretogranin II (fractions 8 and 9) and SNAP-25 (fractions 5 and 6). However, in these cells syntaxin1 distribution changed and in addition to fraction 5 stronger signals appeared in fractions 8 and 9 (Figure 8). The change in syntaxin1 fractions was confirmed through independent blots. Thus, in Munc18-1 knockdown cells, syntaxin1 shows better cofractionation with Secretogranin II, whereas in control cells it demonstrates a better cofractionation with SNAP-25. These results strongly support the finding obtained using immunofluorescence microscopy.

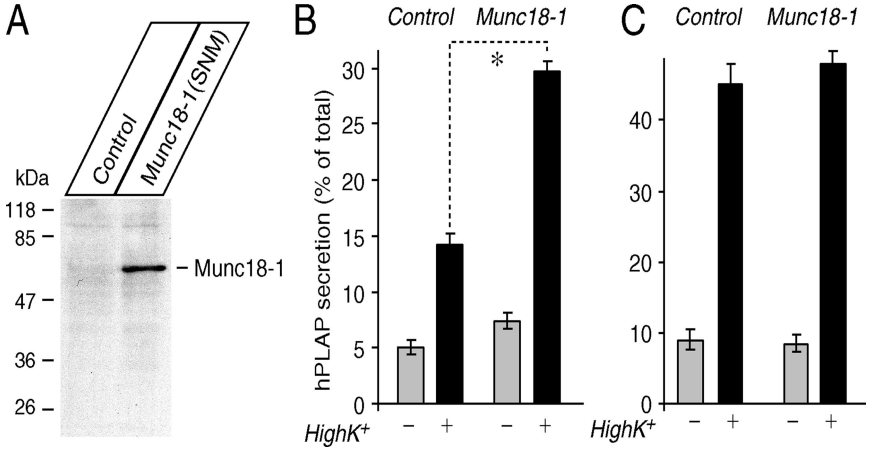

Figure 10. Secretion defects are rescued upon reintroduction of Munc18-1 by transfection. (A) Immunoblot analysis of transfected Munc18-1 in the knockdown (KD43) cells. Thirty micrograms of total homogenates from KD43 cells transfected with the empty plasmid (control) or the Munc18-1 expression plasmid (Munc18-1(SNM)) were analyzed by SDS-PAGE and immunoblotting using anti-Munc18-1. (B) Secretion of NPY-hPLAP from the knockdown (KD43) cells that were transfected with the control plasmid or the Munc18-1 expression plasmid. *$p < 0.01$; a statistically significant difference. Error bar, SEM (n = 9). (C) Secretion of NPY-hPLAP from the control (C1) cells that were transfected with the control plasmid or the Munc18-1 expression plasmid. Error bar, SEM (n = 9).

Expression of Munc18-1 Restores Plasma Membrane Localization of Syntaxin1

To examine whether mislocalized syntaxin1 is truly attributable to down-regulation of Munc18-1, we conducted rescue experiments. Munc18-1 reintroduction was accomplished through the transfection of the Munc18 knockdown (KD43) cells with the Munc18-1 expression constructs. To allow Munc18-1 to be expressed in the KD43 cells, these expression constructs contain SNMs within the sequence region of rat Munc18-1 targeted by the knockdown plasmid (see *Materials and Methods*). We prepared two different Munc18-1 expression constructs: the first being the pCMV-Munc18-1(SNM)-IRES-EGFP construct that expresses Munc18-1 and EGFP as separate proteins where EGFP works as a marker of successful transfection. The other is the pCMV-Munc18-1(SNM)-Emerald GFP construct that expresses Munc18-1 as an Emerald GFP-fusion protein. We found that remarkably the syntaxin1 mislocalization was almost completely rescued upon reintroduction of Munc18-1 into knockdown cells by these constructs (Figure 9). Figure 9A shows representative images of undifferentiated KD43 cells successfully transfected with pCMV-Munc18-1 (SNM)-IRES-EGFP along with untransfected KD43 cells in Figure 9B. The same pixel intensity analysis of syntaxin1 localization used in Figure 3 was repeated on this group of cells and the results are summarized in Figure 9C. As shown in the figure there is a significant increase in syntaxin localization ratios (Student's *t* test, $t_{30} = 8.56$, $p < 0.01$) indicating the ability of transfected Munc18-1 to rescue the syntaxin mislocalization phenotype within Munc18-1 KD43 cells.

We also differentiated the transfected KD43 cells and found the dramatic disappearance of the perinuclear staining of syntaxin1 together with concomitant elevations in plasma membrane staining in the transfected KD43 cells. However, nearby untransfected cells still showed the perinuclear accumulation of syntaxin1 (Figure 9D). Virtually identical results were obtained upon transfection of Munc18-1 fused with Emerald GFP (Figure 9E). One notable difference was that unfused GFP was expressed everywhere in the cell including the nucleus, whereas Munc18-1 fused GFP was only expressed in the cytoplasm. This rescue of syntaxin1 mislocalization upon reintroduction of Munc18-1 confirms a critical role for Munc18-1 in facilitating the plasma membrane localization of syntaxin1.

Expression of Munc18-1 Restores Secretion Defects

We also examined whether Munc18-1 expression by transfection can restore secretion. When we transfected the Munc18-1 knockdown (KD43) cells with pCMV-Munc18-1(SNM), we could detect the expression of transfected Munc18-1(SNM) by immunoblot, whereas the KD43 cells transfected with empty plasmid (pCMV5) did not show significant immunoreactivity of Munc18-1 (Figure 10A). Nevertheless, the transfection rate judged by GFP expression from the Munc18-1-Emerald GFP construct was only ~5–40% (data not shown), not 100%. Therefore, we relied on a cotransfection assay using a reporter plasmid for transfection. This assay originally used human growth hormone expression plasmid as a reporter (Wick *et al.,* 1993; Sugita, 2004). We have recently developed a new plasmid that allows the expression of neuropeptide Y (NPY) fused with a soluble domain (residues 18–506) of human placental alkaline phosphatase (hPLAP; Fujita *et al.,* 2007; Li *et al.,* 2007). NPY-hPLAP is secreted in a Ca^{2+}-dependent manner, and both the levels of NPY-hPLAP secreted from the cells as well as that retained in the cells are easily quantified by measurements of the heat-stable (65°C) alkaline phosphatase activity of hPLAP using the quantitative secretory alkaline phosphatase assay kit (see *Materials and methods*). Thus, NPY-hPLAP can be an ideal reporter for transfection to examine the effect of the transfected protein on secretion. We found that transfection with pCMV-Munc18-1(SNM) enhanced the secretion of cotransfected NPY-hPLAP by ~100% (Figure 10B), which was statistically significant ($t_{16} = 11.8$, $p < 0.01$). Considering that knockdown of Munc18-1 decreased NE secretion by 40–70% (Figure 1), this enhancement is close to the full recovery of secretion. Thus, the secretion defects in Munc18-1 knockdown cells are truly attributable to the reduction of Munc18-1, not the reduction of unrelated proteins. Nevertheless, the secretion level (~30% by high K^+ stimulation) of the rescued KD43 cells still appeared to be lower than the level (~35–50% secretion) exhibited by wild-type PC12 cells in response to the same stimulation. This could be due to the fact that although Munc18-1 transfection rescued the syntaxin1 mislocalization, it did not appear to recover (increase) the reduced expression level of syntaxin1, judged from the comparison of syntaxin1 immunofluorescence intensity between Munc18-1 transfected and untransfected KD43 cells (Figure 9, A and B). Alternatively, the slightly lower secretion level may also be explained by the fact that the coexpression rate of transfected Munc18-1 and NPY-hPLAP is not 100%. In contrast to the knockdown cells, transfection of control (C1) cells with pCMV-Munc18-1(SNM) did not affect the secretion of NPY-hPLAP (Figure 10C; $t_{16} = 0.98$, $p = 0.34$), which reconfirms results from previous Munc18-1 overexpression studies in wild-type PC12 cells (Graham *et al.,* 1997; Schutz *et al.,* 2005), thereby suggesting that Munc18-1 is at saturated levels in control PC12 cells.

DISCUSSION

Regardless of their crucial roles for vesicle trafficking and exocytosis, it remains a mystery *how* the SM proteins, such as Munc18-1, -2, and -3, contribute to these processes. We addressed this issue by generating stable Munc18-1 knockdown cells. The reproduction of secretion defects and dense-core vesicle docking defects in our Munc18-1 knockdown cells (Figures 1 and 2) establishes the credibility of our model system. It proves that the trace levels of residual Munc18-1 left in the Munc18-1 knockdown cells is incapable of fully performing the functional role of Munc18-1 in mammalian cells. Unlike neurons from knockout animals, our Munc18-1 knockdown PC12 cells had no problems in survival or growth. By taking advantage of this relatively healthy condition of the knockdown cells, we could conduct detailed analyses of the localization of syntaxin1 at strongly reduced levels of Munc18-1. We found the dramatic mislocalization of syntaxin1 in both undifferentiated and NGF-differentiated knockdown cells (Figures 3–6). Under NGF-differentiated conditions, clear accumulation of syntaxin1 immunoreactivity in the perinuclear region of the cell was detected (Figures 5 and 6). The finding of mislocalized syntaxin1 by immunofluorescence microscopy was confirmed by subcellular fractionation using equilibrium sucrose density gradient (Figure 8). Furthermore, mislocalized syntaxin1 and reduced secretion were both rescued by the transfection-mediated expression of Munc18-1 (Figures 9 and 10). Thus our work is the demonstration that loss-of-function of endogenous Munc18-1 causes mislocalization of syntaxin1 and supports the previously unconfirmed hypothesis that Munc18-1 is critical for proper trafficking of syntaxin1 (Rowe *et al.,* 1999, 2001).

In previous studies demonstrating the defects in dense-core vesicle docking, the authors implicated Munc18-1 to play a direct functional role in promoting vesicle docking (Voets *et al.*, 2001). The docking defects can now be explained alternatively at least in part by the mislocalized syntaxin1. Such mislocalized syntaxin1 may interact with vesicle SNARE proteins, most likely synaptobrevin/cellubrevin, thereby causing the mislocalization of vesicles as well. Because its discovery, syntaxin1 has been a major candidate responsible for docking of secretory vesicles (Bennett *et al.*, 1992). Although recent analysis of docking of dense-core vesicles in chromaffin cells from SNAP-25 knockout mice (Sorensen *et al.*, 2003) and synaptobrevin/cellubrevin double knockout mice (Borisovska *et al.*, 2005) excluded these two SNARE proteins from their roles in docking of dense-core vesicles, the role for syntaxin1 in docking remains untested. Recently, syntaxin1A knockout mice have been generated but however they failed to reveal any obvious phenotypes in neurotransmitter release (Fujiwara *et al.*, 2006) presumably because of the sustained expression of its close isoform, syntaxin1B, as well as syntaxin2, 3, and 4 (Bennett *et al.*, 1992; Quinones *et al.*, 1999) in these cells. Null mutation of the syntaxin1A orthologue in *Drosophila* causes complete absence of neurotransmitter release and embryonic lethality (Schulze *et al.*, 1995), but it is not known whether synaptic vesicles or dense-core vesicles are docked in these mutants. Nevertheless, we suggest that mislocalized syntaxin1 is the potential cause for the undocking of vesicles in Munc18-1 knockdown cells. However, further work is required to precisely determine whether defects in the docking of vesicles are attributable to mislocalized syntaxin1 or to the absence of Munc18-1.

In addition to localizing syntaxin1 to the plasma membrane, other functional roles for Munc18-1 have been suggested. Studies on the function of the *Drosophila* Munc18-1 orthologue, Rop, using a quantitative overexpression system (Schulze *et al.*, 1994; Wu *et al.*, 1998), found that overexpression of Rop resulted in reduced neurotransmitter release. In addition, they found that overexpression of syntaxin1 also reduced neurotransmitter release, whereas overexpression of both Rop and syntaxin together resulted in almost normal neurotransmitter release. From these results, they proposed the importance of a balance in expression of syntaxin and Rop. As a possible reason for the inhibitory effects observed upon overexpression of Rop, it has been suggested that overexpressed Rop sequesters syntaxins, thereby reducing the amount available to form SNARE complexes with synaptobrevin and SNAP-25. Nonetheless, the loss of function of Munc18-1 or its orthologues have clearly showed that they are required for neurotransmitter release (Hosono *et al.*, 1992; Harrison *et al.*, 1994; Verhage *et al.*, 2000).

Recent biochemical studies suggest that Munc18-1 not only binds to syntaxin1 but also binds the SNARE complex (Zilly *et al.*, 2006; Dulubova *et al.*, 2007). Furthermore, Munc18-1 potently facilitated SNARE-mediated lipid fusion reactions in vitro (Shen *et al.*, 2007). Therefore, Munc18-1 can function as an accelerator of membrane fusion by directly interacting with the SNARE complex. Similarly, Munc18-3 not only interacts with syntaxin4, but also binds to the SNARE complex composed of syntaxin4/SNAP-23/synaptobrevin2 (Latham *et al.*, 2006; Hu *et al.*, 2007). Thus it appears to be a universal feature that the SM proteins interact with the SNARE complexes as well as the specific syntaxins. It is however important to note that the loss-of-function of Munc18-1 affects syntaxin1 (expression level and/or localization) but not SNAP-25 or synaptobrevin2 (Voets *et al.*, 2001; this study). Similarly, knockout of Munc18-3 resulted in a strong reduction in syntaxin4 expression but not in SNAP-23 or synaptobrevin2 (Kanda *et al.*, 2005). Thus at least a component of SM functions is selectively related to syntaxins and not to SNARE proteins in general. It has not been demonstrated that syntaxin4 is mislocalized in Munc18-3–deficient cells. Thus it remains to be seen whether the Munc18 family proteins are universally involved in the trafficking of syntaxins.

Interestingly, we detected substantial expression of Munc18-2 (Hata and Südhof, 1995; Katagiri *et al.*, 1995; Tellam *et al.*, 1995; Halachmi and Lev, 1996; Riento *et al.*, 1996) in PC12 cells, and in addition its expression seemed to be notably elevated in Munc18-1 knockdown cells. Although the expression of Munc18-2 in chromaffin cells has not been examined, it is reasonable to expect its expression based on the similarity between PC12 cells and chromaffin cells. In contrast, the expression of Munc18-2 is undetectable in neurons (Hata and Südhof, 1995). This difference in the expression of Munc18-2 may in fact explain the differences observed in the severity of the release phenotype between neurons and chromaffin cells from Munc18-1 knockout mice. In neurons, neurotransmitter release was completely blocked (Verhage *et al.*, 2000), whereas in chromaffin cells 10–20% of secretion was still detectable (Voets *et al.*, 2001). In fact, it is known that Munc18-2, but not Munc18-3, can bind to syntaxin1 (Hata and Südhof, 1995; Tellam *et al.*, 1995, 1997; Halachmi and Lev, 1996; Riento *et al.*, 1998, 2000; Kauppi *et al.*, 2002).

Although our results clearly establish the importance of Munc18-1 in trafficking syntaxin1 to the plasma membrane, whether the secretion and dense-core vesicle docking deficiencies observed are entirely the result of syntaxin1 mislocalization still remains speculative. However, the viability of the knockdown cells in our model allows us to conduct further experiments that would elucidate the importance of plasma membrane syntaxin1 localization in vesicle docking and subsequent exocytosis. In the case that dense-core vesicle docking and syntaxin1 localization are the result of independent actions of Munc18-1, it would almost certainly be that such independent functions of Munc18-1 are regulated by different domains within the protein. In the case that both dense-core vesicle docking deficiency and syntaxin1 mislocalization are simultaneously rescued by the reintroduction of the syntaxin1 binding domain of Munc18-1 or various Munc18-1 mutants, it would strongly suggest that the dense-core vesicle docking defects observed were the direct result of syntaxin1 mislocalization.

ACKNOWLEDGMENTS

We thank Drs. R. Agami, A. Miyawaki, R. Fernández-Chacón, W. Han, R. Jahn, and R. Bremner for providing reagents for this study. We also thank Mr. Steven Doyle for his excellent technical help in electron microscopy that was conducted in Microscopy Imaging Laboratory at the University of Toronto. We also thank Dr. Tony Collins for his excellent help in confocal microscopy conducted in the Wright Cell Imaging Facility at Toronto Western Research Institute. We thank Drs. Michael Tymianski and Xiujun Sun for their help in the use of Luminescent Image Analyzer. We thank members of Sugita lab for critically reading the manuscript. This research was supported by the Canada Research Chair program, Natural Sciences and Engineering Research Council of Canada (456042) and the Canadian Institute of Health Research (MOP-57825 and MOP-64465).

REFERENCES

Barnstable, C. J., Hofstein, R., and Akagawa, K. (1985). A marker of early amacrine cell development in rat retina. Brain Res. *352*, 286–290.

Bennett, M. K., Calakos, N., and Scheller, R. H. (1992). Syntaxin: a synaptic protein implicated in docking of synaptic vesicles at presynaptic active zones. Science *257*, 255–259.

Borisovska, M., Zhao, Y., Tsytsyura, Y., Glyvuk, N., Takamori, S., Matti, U., Rettig, J., Südhof, T., and Bruns, D. (2005). v-SNAREs control exocytosis of vesicles from priming to fusion. EMBO J. *24*, 2114–2126.

Brummelkamp, T. R., Bernards, R., and Agami, R. (2002). A system for stable expression of short interfering RNAs in mammalian cells. Science *296*, 550–553.

de Wit, H., Cornelisse, L. N., Toonen, R. F., and Verhage, M. (2006). Docking of secretory vesicles is syntaxin dependent. PLoS ONE *1*, e126.

Dulubova, I., Khvotchev, M., Liu, S., Huryeva, I., Südhof, T. C., and Rizo, J. (2007). Munc18-1 binds directly to the neuronal SNARE complex. Proc. Natl. Acad. Sci. USA *104*, 2697–2702.

Fisher, R. J., Pevsner, J., and Burgoyne, R. D. (2001). Control of fusion pore dynamics during exocytosis by Munc18. Science *291*, 875–878.

Fujita, Y. *et al.* (2007). Ca^{2+}-dependent activator for secretion 1 is critical for constitutive and regulated exocytosis, but not for loading of transmitters into dense-core vesicles. J. Biol. Chem. *282*, 21392–21403.

Fujiwara, T., Mishima, T., Kofuji, T., Chiba, T., Tanaka, K., Yamamoto, A., and Akagawa, K. (2006). Analysis of knock-out mice to determine the role of HPC-1/syntaxin 1A in expressing synaptic plasticity. J. Neurosci. *26*, 5767–5776.

Graham, M. E., Sudlow, A. W., and Burgoyne, R. D. (1997). Evidence against an acute inhibitory role of nSec-1 (munc-18) in late steps of regulated exocytosis in chromaffin and PC12 cells. J. Neurochem. *69*, 2369–2377.

Garcia, E. P., Gatti, E., Butler, M., Burton, J., and De Camilli, P. (1994). A rat brain Sec1 homologue related to Rop and UNC18 interacts with syntaxin. Proc. Natl. Acad. Sci. USA *91*, 2003–2007.

Halachmi, N., and Lev, Z. (1996). The Sec1 family: a novel family of proteins involved in synaptic transmission and general secretion. J. Neurochem. *66*, 889–897.

Harrison, S. D., Broadie, K., van de Goor, J., and Rubin, G. M. (1994). Mutations in the *Drosophila* Rop gene suggest a function in general secretion and synaptic transmission. Neuron *13*, 555–566.

Hata, Y., and Südhof, T. C. (1995). A novel ubiquitous form of Munc-18 interacts with multiple syntaxins. Use of the yeast two-hybrid system to study interactions between proteins involved in membrane traffic. J. Biol. Chem. *270*, 13022–13028.

Hata, Y., Slaughter, C. A., and Südhof, T. C. (1993). Synaptic vesicle fusion complex contains unc-18 homologue bound to syntaxin. Nature *366*, 347–351.

Heeroma, J. H., Roelandse, M., Wierda, K., van Aerde, K. I., Toonen, R. F., Hensbroek, R. A., Brussaard, A., Matus, A., and Verhage, M. (2004). Trophic support delays but does not prevent cell-intrinsic degeneration of neurons deficient for munc18–1. Eur. J. Neurosci. *20*, 623–634.

Hosono, R., Hekimi, S., Kamiya, Y., Sassa, T., Murakami, S., Nishiwaki, K., Miwa, J., Taketo, A., and Kodaira, K. I. (1992). The unc-18 gene encodes a novel protein affecting the kinetics of acetylcholine metabolism in the nematode *Caenorhabditis elegans*. J. Neurochem. *58*, 1517–1525.

Hu, S. H., Latham, C. F., Gee, C. L., James, D. E., and Martin, J. L. (2007). Structure of the Munc18c/Syntaxin4 N-peptide complex defines universal features of the N-peptide binding mode of Sec1/Munc18 proteins. Proc. Natl. Acad. Sci. USA *104*, 8773–8778.

Kanda, H., Tamori, Y., Shinoda, H., Yoshikawa, M., Sakaue, M., Udagawa, J., Otani, H., Tashiro, F., Miyazaki, J., and Kasuga, M. (2005). Adipocytes from Munc18c-null mice show increased sensitivity to insulin-stimulated GLUT4 externalization. J. Clin. Invest. *115*, 291–301.

Katagiri, H. *et al.* (1995). A novel isoform of syntaxin-binding protein homologous to yeast Sec1 expressed ubiquitously in mammalian cells. J. Biol. Chem. *270*, 4963–4966.

Kauppi, M., Wohlfahrt, G., and Olkkonen, V. M. (2002). Analysis of the Munc18b-syntaxin binding interface. Use of a mutant Munc18b to dissect the functions of syntaxins 2 and 3. J. Biol. Chem. *277*, 43973–43979.

Latham, C. F. *et al.* (2006). Molecular dissection of the Munc18c/syntaxin4 interaction: implications for regulation of membrane trafficking. Traffic *7*, 1408–1419.

Li, G., Lee, D., Wang, L., Khvotchev, M., Chiew, S. K., Arunachalam, L., Collins, T., Feng, Z. P., and Sugita, S. (2005). N-terminal insertion and C-terminal ankyrin-like repeats of α-latrotoxin are critical for Ca^{2+}-dependent exocytosis. J. Neurosci. *25*, 10188–10197.

Li, G., Han, L., Chou, T. C., Fujita, Y., Arunachalam, L., Xu, A., Wong, A., Chiew, S. K., Wan, Q., Wang, L., and Sugita, S. (2007). RalA and RalB function as the critical GTP sensors for GTP-dependent exocytosis. J. Neurosci. *27*, 190–202.

Nagai, T., Ibata, K., Park, E. S., Kubota, M., Mikoshiba, K., and Miyawaki, A. (2002). A variant of yellow fluorescent protein with fast and efficient maturation for cell-biological applications. Nat. Biotechnol. *20*, 87–90.

Oh, E., Spurlin, B. A., Pessin, J. E., and Thurmond, D. C. (2005). Munc18c heterozygous knockout mice display increased susceptibility for severe glucose intolerance. Diabetes *54*, 638–647.

Peters, J. M., Walsh, M. J., and Franke, W. W. (1990). An abundant and ubiquitous homo-oligomeric ring-shaped ATPase particle related to the putative vesicle fusion proteins Sec18p and NSF. EMBO J. *9*, 1757–1767.

Pevsner, J., Hsu, S. C., and Scheller, R. H. (1994). n-Sec1, a neural-specific syntaxin-binding protein. Proc. Natl. Acad. Sci. USA *91*, 1445–1449.

Quinones, B., Riento, K., Olkkonen, V. M., Hardy, S., and Bennett, M. K. (1999). Syntaxin 2 splice variants exhibit differential expression patterns, biochemical properties and subcellular localizations. J. Cell Sci. *112*, 4291–4304.

Reetz, A., Solimena, M., Matteoli, M., Folli, F., Takei, K., and De Camilli, P. (1991). GABA and pancreatic beta-cells: colocalization of glutamic acid decarboxylase (GAD) and GABA with synaptic-like microvesicles suggests their role in GABA storage and secretion. EMBO J. *10*, 1275–1284.

Riento, K., Galli, T., Jansson, S., Ehnholm, C., Lehtonen, E., and Olkkonen, V. M. (1998). Interaction of Munc-18–2 with syntaxin 3 controls the association of apical SNAREs in epithelial cells. J. Cell Sci. *111*, 2681–2688.

Riento, K., Jantti, J., Jansson, S., Hielm, S., Lehtonen, E., Ehnholm, C., Keranen, S., and Olkkonen, V. M. (1996). A sec1-related vesicle-transport protein that is expressed predominantly in epithelial cells. Eur. J. Biochem. *239*, 638–646.

Riento, K., Kauppi, M., Keranen, S., and Olkkonen, V. M. (2000). Munc18-2, a functional partner of syntaxin 3, controls apical membrane trafficking in epithelial cells. J. Biol. Chem. *275*, 13476–13483.

Rowe, J., Corradi, N., Malosio, M. L., Taverna, E., Halban, P., Meldolesi, J., and Rosa, P. (1999). Blockade of membrane transport and disassembly of the Golgi complex by expression of syntaxin 1A in neurosecretion-incompetent cells: prevention by rbSEC1. J. Cell Sci. *112*, 1865–1877.

Rowe, J., Calegari, F., Taverna, E., Longhi, R., and Rosa, P. (2001). Syntaxin 1A is delivered to the apical and basolateral domains of epithelial cells: the role of munc-18 proteins. J. Cell Sci. *114*, 3323–3332.

Schulze, K. L., Broadie, K., Perin, M. S., and Bellen, H. J. (1995). Genetic and electrophysiological studies of *Drosophila* syntaxin-1A demonstrate its role in nonneuronal secretion and neurotransmission. Cell *80*, 311–320.

Schulze, K. L., Littleton, J. T., Salzberg, A., Halachmi, N., Stern, M., Lev, Z., and Bellen, H. J. (1994). Rop, a *Drosophila* homolog of yeast Sec1 and vertebrate n-Sec1/Munc-18 proteins, is a negative regulator of neurotransmitter release in vivo. Neuron *13*, 1099–1108.

Schutz, D., Zilly, F., Lang, T., Jahn, R., and Bruns, D. (2005). A dual function for Munc-18 in exocytosis of PC12 cells. Eur. J. Neurosci. *21*, 2419–2432.

Shen, J., Tareste, D. C., Paumet, F., Rothman, J. E., and Melia, T. J. (2007). Selective activation of cognate SNAREpins by Sec1/Munc18 proteins. Cell *128*, 183–195.

Sollner, T., Whiteheart, S. W., Brunner, M., Erdjument-Bromage, H., Geromanos, S., Tempst, P., and Rothman, J. E. (1993). SNAP receptors implicated in vesicle targeting and fusion. Nature *362*, 318–324.

Sorensen, J. B., Nagy, G., Varoqueaux, F., Nehring, R. B., Brose, N., Wilson, M. C., and Neher, E. (2003). Differential control of the releasable vesicle pools by SNAP-25 splice variants and SNAP-23. Cell *114*, 75–86.

Sugita, S. (2004). Human growth hormone co-transfection assay to study molecular mechanisms of neurosecretion in PC12 cells. Methods *33*, 267–272.

Sugita, S., Janz, R., and Südhof, T. C. (1999). Synaptogyrins regulate Ca^{2+}-dependent exocytosis in PC12 cells. J. Biol. Chem. *274*, 18893–18901.

Sugita, S., and Südhof, T. C. (2000). Specificity of Ca^{2+}-dependent protein interactions mediated by the C2A domains of synaptotagmins. Biochemistry *39*, 2940–2949.

Tellam, J. T., McIntosh, S., and James, D. E. (1995). Molecular identification of two novel Munc-18 isoforms expressed in non-neuronal tissues. J. Biol. Chem. *270*, 5857–5863.

Tellam, J. T., Macaulay, S. L., McIntosh, S., Hewish, D. R., Ward, C. W., and James, D. E. (1997). Characterization of Munc-18c and syntaxin-4 in 3T3–L1 adipocytes: putative role in insulin-dependent movement of GLUT-4. J. Biol. Chem. *272*, 6179–6186.

Toonen, R. F., de Vries, K. J., Zalm, R., Südhof, T. C., and Verhage, M. (2005). Munc18-1 stabilizes syntaxin 1, but is not essential for syntaxin 1 targeting and SNARE complex formation. J. Neurochem. *93*, 1393–1400.

Tooze, S. A. (1998). Biogenesis of secretory granules in the trans-Golgi network of neuroendocrine and endocrine cells. Biochim. Biophys. Acta *1404*, 231–244.

Verhage, M. *et al.* (2000). Synaptic assembly of the brain in the absence of neurotransmitter secretion. Science *287*, 864–869.

Voets, T., Toonen, R. F., Brian, E. C., de Wit, H., Moser, T., Rettig, J., Südhof, T. C., Neher, E., and Verhage, M. (2001). Munc18-1 promotes large dense-core vesicle docking. Neuron *31*, 581–591.

Wang, L., Li, G., and Sugita, S. (2004). RalA-exocyst interaction mediates GTP-dependent exocytosis. J. Biol. Chem. *279*, 19875–19881.

Wang, L., Li, G., and Sugita, S. (2005). A central kinase domain of type I phosphatidylinositol phosphate kinases is sufficient to prime exocytosis: isoform specificity and its underlying mechanism. J. Biol. Chem. *280*, 16522–16527.

Weimer, R. M., Richmond, J. E., Davis, W. S., Hadwiger, G., Nonet, M. L., and Jorgensen, E. M. (2003). Defects in synaptic vesicle docking in unc-18 mutants. Nat. Neurosci. *6*, 1023–1030.

Wick, P. F., Senter, R. A., Parsels, L. A., Uhler, M. D., and Holz, R. W. (1993). Transient transfection studies of secretion in bovine chromaffin cells and PC12 cells. Generation of kainate-sensitive chromaffin cells. J. Biol. Chem. *268*, 10983–10989.

Wu, M. N., Littleton, J. T., Bhat, M. A., Prokop, A., and Bellen, H. J. (1998). ROP, the *Drosophila* Sec1 homolog, interacts with syntaxin and regulates neurotransmitter release in a dosage-dependent manner. EMBO J. *17*, 127–139.

Zilly, F. E., Sorensen, J. B., Jahn, R., and Lang, T. (2006). Munc18-bound syntaxin readily forms SNARE complexes with synaptobrevin in native plasma membranes. PLoS Biol. *4*, e330.